International Journal of Cardiology xxx (2017) xxx–xxx

Contents lists available at ScienceDirect

International Journal of Cardiology

journal homepage: www.elsevier.com/locate/ijcard

c-Jun dimerization protein 2 (JDP2) deficiency promotes cardiac hypertrophy and dysfunction in response to pressure overload

R. Kalfon [a], T. Haas [b], R. Shofti [b], J.D. Moskovitz [a], O. Schwartz [c], E. Suss-Toby [c], A. Aronheim [a,*]

[a] Department of Cell Biology and Cancer Science, B. Rappaport Faculty of Medicine, Technion-Israel Institute of Technology, Haifa, Israel
[b] The Pre-Clinical Research Authority Unit, The Technion, Israel Institute of Technology, Haifa, Israel
[c] Biomedical Core Facility, Bio-imaging Center, B. Rappaport Faculty of Medicine, Technion-Israel Institute of Technology, Haifa, Israel

ARTICLE INFO

Article history:
Received 28 April 2017
Received in revised form 23 August 2017
Accepted 29 August 2017
Available online xxxx

1. Introduction

The c-Jun dimerization protein 2, JDP2, is a member of the basic leucine zipper (bZIP) superfamily [1]. JDP2 is constitutively expressed in all cells tested [2]. As a homodimer, JDP2 typically suppresses transcription through binding to CRE and TRE DNA elements found in the promoters of numerous genes by recruitment of histone deacetylases [3]. Alternatively, JDP2 associates with other members of the bZIP family. JDP2 is able to activate transcription when associated with CHOP10 [4] or as a co-activator of the steroid hormone receptors [5]. JDP2 shares a high degree of homology with Activating Transcription Factor 3, ATF3, especially within the bZIP domain; thus it is not surprising that ATF3 and JDP2 share similar target genes and cellular functions [3,6]. Furthermore, JDP2 is able to suppress ATF3 transcription through a composite TRE site located within the ATF3 promoter [7].

ATF3 expression in the heart is highly induced as a result of numerous cardiac insults [8]. Although much research has been done in various cardiac models, the role of ATF3 expression in the heart is controversial [9–13]. Transgenic mice with embryonic cardiomyocytes' specific expression of either JDP2 or ATF3 resulted in enlarged atria and a lethal phenotype [14–16]. JDP2 expression in cardiomyocytes protects against hypertrophy and apoptosis in vitro [17]. Importantly, adult ATF3 expression resulted in a hypertrophic heart phenotype with increased fibrosis and cardiac dysfunction [16]. In a pressure overload model using phenylephrine infusion, ATF3 expression has been correlated with maladaptive cardiac remodeling [18,19]. However, using transverse aortic constriction (TAC) and angiotensin II infusion models, ATF3 deficiency was shown to promote heart failure and cardiac dysfunction [20,21]. In addition, we have shown through an obesity induced type II diabetes model that ATF3 expression preserves homeostasis and preserves cardiac function [22]. Most importantly, patients with heart failure display high levels of cardiac ATF3 expression [20,21], suggesting that ATF3 may play a role in cardiac remodeling processes, however, whether ATF3 in the failing heart is part of an adaptive or a maladaptive process needs further research [12]. To partially resolve the aforementioned discrepancies, we studied the role of JDP2 expression in cardiac remodeling process following TAC. ATF3 is a known JDP2 target gene [7]. In the absence of JDP2, ATF3 expression is elevated. Thus, we used C57Bl/6 mice harboring whole body knockout (KO) of either JDP2 or ATF3 and examined cardiac remodeling processes in normal growth and following pressure overload model. Our finding is consistent with the notion that ATF3 expression is a cardiac maladaptive process following TAC while JDP2 expression is an adaptive mechanism that lowers ATF3 expression and promotes activation of the p38 signaling pathway.

2. Materials and methods

2.1. Mice

This study was carried out in strict accordance with the Guide for the Care and Use of Laboratory Animals of the National Institute of Health. In addition, our protocol was approved by the Committee of the Ethics of Animal Experiments of the Technion. Mice strains used in this study: whole-body ATF3 KO (ATF3-KO) [23] and JDP2 KO (JDP2-KO) [24], ATF3-flox ($ATF3^{f/f}$) [25], and αMHC-Cre [26]. All mice genotypes are on C57Bl/6 background. Male mice were used in all the experiments.

2.2. TAC-induced cardiac hypertrophy

Studies were conducted at the Technion, Israel Institute of Technology, Faculty of Medicine, Haifa, Israel, after obtaining approval from the institute's care and use committee for animal experimentation. All proceedings complied with the Animal Welfare Act of 1966 (P.L. 89–544), as amended by the Animal Welfare Act of 1970 (P.L.91–579) and 1976 (P.L. 94–279). TAC procedure was done according to the previously described protocol [27,28] using a 27 G blunt needle to create a standardized constriction of the aorta. All TAC procedures were performed by Dr. R. Shofti which was blinded to the mice genotype.

2.3. Echocardiography

Mice were anesthetized with 1% of isoflurane and kept on a 37 °C heated plate throughout the procedure. An echocardiography was performed four weeks following TAC using a Vevo2100 micro-ultrasound imaging system (VisualSonics, Fujifilm) which was equipped with 13–38 MHz (MS 400) and 22–55 MHz (MS550D) linear array transducers. Those performing echocardiography and data analysis were blinded to the mice

* Corresponding author at: Department of Cell Biology and Cancer Science, The B. Rappaport Faculty of Medicine, Technion-Israel Institute of Technology, 7th Efron St. Bat-Galim, Haifa 31096, Israel.
E-mail address: aronheim@tx.technion.ac.il (A. Aronheim).

http://dx.doi.org/10.1016/j.ijcard.2017.08.074

genotype. Cardiac size, shape, and function were analyzed by conventional two-dimensional imaging and M-Mode recordings. Maximal left ventricles end-diastolic (LVDd) and end-systolic (LVDs) dimensions were measured in short-axis M-mode images. Fractional shortening (FS) was calculated as follows: FS (%) = [(LVDd − LVDs) / LVDd] × 100. All values were based on the average of at least five measurements.

2.4. MRI hardware and animal monitoring

A MRI was performed on a 9.4T bore scanner (Bruker Biospec, Ettlingen, Germany), using a cylindrical volume coil (86 mm inner diameter) for signal excitation and a single channel surface coil (20 mm diameter) for signal reception. The animal was anesthetized with a concentration of 0.5–1.5% isoflurane, and supplemented with oxygen (0.5 l/min). Respiration was monitored during imaging (Small Animal Instruments, Stony Brook, New York, NY) and body temperature was maintained using thermostat-regulated circulating hot water.

2.5. Cardiac MR (CMR) sequences

The mice were scanned using cine FLASH sequence, acquired from the self-gating technique IntraGate (Bruker BioSpin MRI, Ettlingen, Germany). The performed CMR protocol comprised of three sets of scans: (i) Single slice Long Axis view, for general evaluation of the heart structure and accurate planning of the subsequent scans; (ii) Single slice two chamber Short Axis view, perpendicular to LV walls, at the level of the papillary muscles, and (iii) Contiguous multi slices two chamber Short Axis view for entire LV coverage.

2.6. Cardiac MR sequences parameters

i. Single slice Long Axis view. 1 mm thickness, FOV = 3 × 3 cm, matrix dimension = 400 × 400, spatial resolution = 75 × 75 μm^2, repetition/echo time (TR/TE) = 6.5/3.2 ms, number of repetitions = 100, 10 cardiac movie frames (cardiac phases).
ii. Single slice two chamber Short Axis view. 0.7 mm thickness, FOV = 3 × 3cm, matrix dimension = 400 × 400, spatial resolution = 75 × 75 μm^2, repetition/echo time (TR/TE) = 6.5/3.2 ms, number of repetitions = 150, 15 cardiac movie frames (cardiac phases).
iii. Multi slices two chamber Short Axis view. Contiguous 9–12 slices, depending on heart size, 0.7 mm thickness, FOV = 3 × 3cm, matrix dimension = 400 × 400, spatial resolution = 75 × 75 μm^2, repetition/echo time (TR/TE) = 81–120/3.2 ms (depending on slices number), number of repetitions = 120, 15 cardiac movie frames (cardiac phases). The maximal acquisition time for each animal was ~40 min.

2.7. MRI image analysis

Image analysis was performed using Segment software (Medviso AB, Lund, Sweden) [29]. Manual segmentation of the endocardium and epicardium of the LV was performed to measure LV mass and LV functional parameters – end-systolic and end-diastolic (ESV and EDV, respectively) volumes. Ejection fraction (EF) was calculated as EF (%) = [(EDV − ESV) / EDV] × 100.

2.8. Heart harvesting

At endpoint, mice were anesthetized, weighed and sacrificed. Hearts were excised, and ventricles were weighed and then divided into three pieces that were used for protein extraction, RNA purification, and histological analysis.

2.9. mRNA extraction

mRNA was purified from ventricles using an Aurum total RNA fatty or fibrous tissue kit (#732-6830, Bio-Rad) according to the manufacturer's instructions.

2.10. Quantitative real time PCR (qRT-PCR(

cDNA was synthesized from 800 ng of purified mRNA derived from the ventricles. Purified mRNA was added to a total reaction mix of high-capacity cDNA reverse transcription kit (#4368814, Applied Biosystems) in a final volume of 20 μl. Real-time PCR was performed using Rotor-Gene 6000TM (Corbett) equipment with absolute blue SYBER green ROX mix (Thermo Scientific AB-4162/B). Serial dilutions of a standard sample were included for each gene to generate a standard curve. Values were normalized to β2 microglobulin expression levels. The primer sequences are shown in Supplemental Table 1.

2.11. Fibrosis staining

Heart tissue was fixed in 4% formaldehyde overnight, embedded in paraffin, serially sectioned at 10 μm intervals, and then mounted on slides. Masson's trichrome staining was performed according to the standard protocol. Images were acquired by using Virtual Microscopy (Olympus). The percent of the interstitial fibrosis was determined as the ratio of the fibrosis area to the total area of the heart section using Image Pro Plus software [21].

2.12. Western blot analysis and quantification

Harvested tissues were homogenized in RIPA buffer (PBS containing 1% NP-40, 5 mg/ml Na-deoxycholate, 0.1% SDS) and supplemented with protease inhibitor cocktail (P-8340, Sigma Aldrich). Homogenization was performed at 4 °C using the Bullet Blender homogenizer (BBX24; Next advance) according to the manufacturer's instructions as previously described [13].

2.13. Antibodies

The primary antibodies used: anti-α-tubulin (Cat # T-9026), anti-phospho-ERK (Cat# M-9692), anti-phospho-JNK (Cat# J-4644) and anti-JNK (Cat# J-4750) were all purchased from Sigma Aldrich. Anti-p38 (Cat# 9212), anti-phospho-p38 (Cat# 9211) and anti-ERK (Cat# 9102) were purchased from Cell signaling.

2.14. Apoptosis

Apoptosis was performed using in situ cell death detection assay kit (Roche Inc.) according to the manufacturer instructions.

2.15. Statistics

Our data is expressed as means ± SE. The comparison between several means was analyzed by one-way ANOVA followed by Tukey's post hoc analysis. All statistical analyses were performed using GraphPad Prism 5 software (La Jolla, CA). A P value ≤0.05 was accepted as statistically significant.

3. Results

3.1. JDP2-KO derived hearts display the highest ventricles/body weight ratio in control and TAC operated mice

To assess the role of the JDP2 and ATF3 in TAC mediated cardiac hypertrophy, we used C57Bl/6 mice with whole body deletion of either of the genes. The hearts from control mice were harvested at 20 weeks of age. JDP2-KO hearts displayed the highest ratio of ventricles/body weight (Vw/Bw) compared to aged match ATF3-KO and wild type mice (Fig. 1A). Eight weeks following TAC operation the Vw/Bw ratio of all mice was significantly increased (Fig. 1A and B). While wild type and JDP2-KO hearts showed the highest increase in the percentage of Vw/Bw ratio as compared with the non-operated mice counterparts (58% and 63% respectively), ATF3-KO mice showed a modest increase in Vw/Bw ratio (32%, Fig. 1A and B). Although the percent change for JDP2-KO and wild type following TAC are similar, the hearts derived from JDP2-KO mice reached the highest Vw/Bw (7.5). This is attributed to the high Vw/Bw ratio in control JDP2-KO mice (4.8) compared to wild type control mice (3.8).

3.2. JDP2-KO mice display increased hypertrophic markers

We next examined the cardiac expression of various genetic markers as an indication of a stressed heart using quantitative RT-PCR. All TAC-operated mice displayed a significant increase in hypertrophic markers ANP, BNP and βMHC compared to control mice (Fig. 1 C–E). Both ATF3-KO and JDP2-KO mice displayed higher levels of ANP and BNP in control mice but only the JDP2-KO mice reached statistical significance. Following TAC operation, the levels of both ANP and BNP were two fold higher in JDP2-KO mice as compared with the wild type mice counterparts, while the level of ANP and BNP transcript in the hearts derived from ATF3-KO mice following TAC-operation were the lowest (Fig. 1 C–D). While the level of βMHC transcript was the highest in ATF3-KO control mice, the level of βMHC was significantly lower in ATF3-KO mice as compared with wild type and JDP2-KO mice following TAC (Fig. 1E). No significant difference was observed between wild type and JDP2-KO mice (Fig. 1E).

Collectively, JDP2-KO mice displayed the highest expression of hypertrophic markers in control mice as well as following TAC. In addition, ATF3-KO mice showed a modest change in hypertrophic gene expression as compared with both wild type and JDP2-KO mice.

Please cite this article as: R. Kalfon, et al., c-Jun dimerization protein 2 (JDP2) deficiency promotes cardiac hypertrophy and dysfunction in response to pressure overload, Int J Cardiol (2017), http://dx.doi.org/10.1016/j.ijcard.2017.08.074

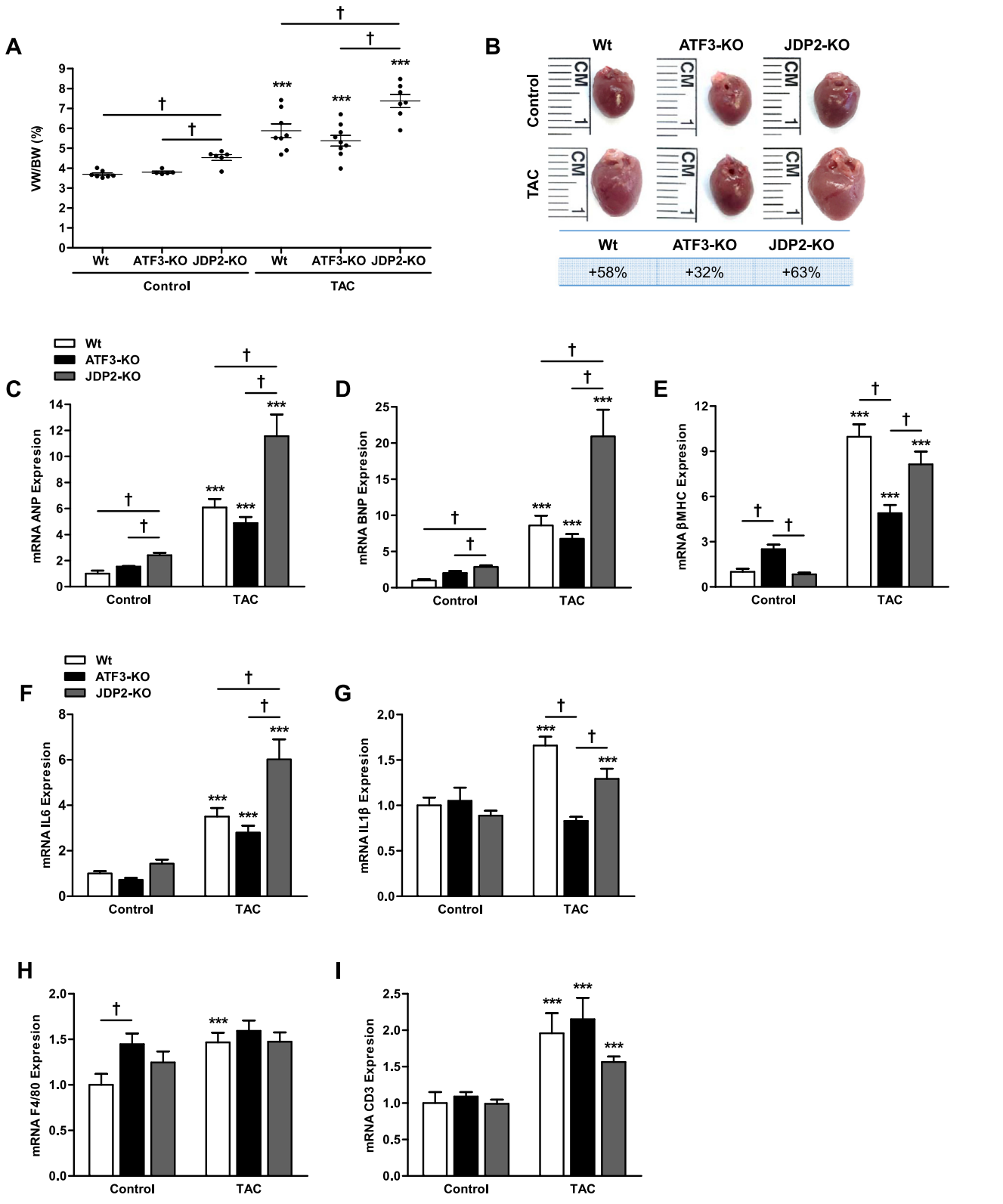

Fig. 1. JDP2-KO mice display increased cardiac hypertrophy following TAC. Cardiac hypertrophy was induced by pressure overload (TAC). Following 8 weeks of TAC, mice were sacrificed and hearts were excised. (A) The ratio of ventricles weigh (Vw) to mouse body weight (Bw) Vw/Bw (mg/gr) is shown. (B) Representative pictures of control and TAC-operated mice hearts of each genotype. The percentage increase in Vw/Bw ratio is shown at the bottom. (C—H) mRNA was extracted from ventricles and the expression level of cardiac remodeling markers were measured by qRT-PCR. Expression levels are presented as relative values (compared to wild type control mice, determined as 1). The expression levels of the following gene markers are shown: C. ANP D. BNP E. βMHC. F. IL-6 G. IL1-β. H. F4/80. I. CD3. The results represent the means ± SE ($n = 6–8$/group). $^{***}P \leq 0.05$, control vs. TAC; $^{\dagger}P \leq 0.05$, difference between genotypes.

Please cite this article as: R. Kalfon, et al., c-Jun dimerization protein 2 (JDP2) deficiency promotes cardiac hypertrophy and dysfunction in response to pressure overload, Int J Cardiol (2017), http://dx.doi.org/10.1016/j.ijcard.2017.08.074

3.3. JDP2-KO mice display increased inflammatory markers

We next examined the expression level of the inflammatory cytokines, interleukin 6 (IL-6) (Fig. 1F) and IL-1β (Fig. 1G). No significant difference in IL-6 expression was observed in control mice. While IL-6 level was significantly increased following TAC-operation in all three genotypes, JDP2-KO mice showed a two-fold increase in IL-6 expression (Fig. 1F). The expression of IL-1β, was expressed in similar levels in control mice, yet, following TAC, IL-1β expression was found to be the highest in wild type and JDP2-KO mice as compared to ATF3-KO mice (Fig. 1G). Macrophage and T cells infiltration as indicated by F4/80 and CD3 expression, respectively, were similar following TAC in all three genotypes (Fig. 1H-I). Suggesting that the differences observed in the pathology of 8-week TAC model between the various genotypes, are not due to altered macrophages and T cells recruitment to the heart.

Collectively, JDP2-KO mice display an increased inflammatory response following TAC operation while no significant difference was observed, at least in part, between wild type and ATF3-KO mice.

3.4. 3.4 JDP2-KO mice display increased fibrosis

We next examined several hallmarks of fibrosis markers collα, cTGF and TGFβ (Fig. 2 A–C). The levels of all fibrosis markers were significantly higher in the hearts derived from either JDP2-KO or ATF3-KO control mice groups compared to wild type mice counterparts (Fig. 2 A–C). Importantly, following TAC, the hearts derived from JDP2-KO mice displayed the highest expression levels in these three fibrosis markers. In addition, the hearts derived from ATF3-KO showed the lowest expression of fibrosis markers compared to all other genotypes following TAC (Fig. 2 A–C). The fibrosis modifying enzymes matrix metallopeptidase 2 and 9 and their tissue inhibitor metalloproteinase (TIMP) are responsible for regulating the collagen deposition in a tissue. The expression levels of these enzymes were significantly the highest in control and TAC-operated JDP2-KO mice (Fig. 2 D–F). Nevertheless, wild type and ATF3-KO mice consistently displayed the lowest levels of these markers following TAC operation.

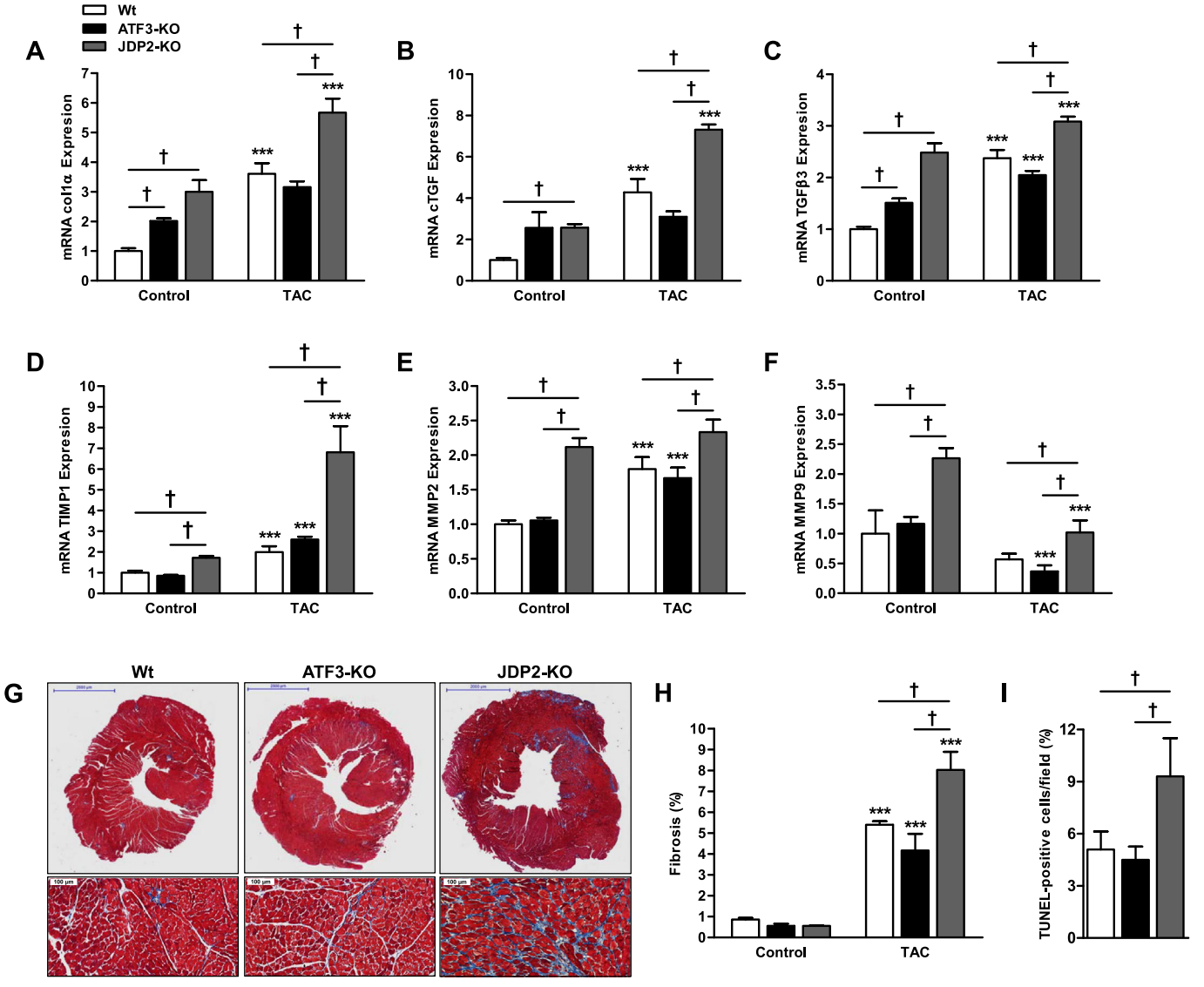

Fig. 2. JDP2-KO mice display higher level of fibrosis in the heart. Cardiac hypertrophy was induced by pressure overload (TAC). Following 8 weeks of TAC, mice were sacrificed and hearts were excised. (A–F) mRNA was extracted from ventricles and the expression levels of the following fibrosis markers were measured by qRT-PCR: A. Col1α B. cTGF C. TGFβ3 D. TIMP1 E. MMP2 F. MMP9. Expression levels are presented as relative values (compared to wild type control mice, determined as 1). The results represent the means ± SE (n = 6–8/group). (G) Representative paraffin-embedded heart sections stained with Masson's trichrome to visualize fibrosis. (H) Quantification of the level of fibrosis (%) stained by Masson's trichrome. (I) Quantification of apoptotic stained cardiomyocytes in TAC-operated mice hearts. The results represent the means ± SE (n = 4–5/group). $^{***}P \le 0.05$, control vs. TAC; $^{\dagger}P \le 0.05$, difference between genotypes.

Please cite this article as: R. Kalfon, et al., c-Jun dimerization protein 2 (JDP2) deficiency promotes cardiac hypertrophy and dysfunction in response to pressure overload, Int J Cardiol (2017), http://dx.doi.org/10.1016/j.ijcard.2017.08.074

Next, fibrosis was examined histologically by Masson's trichrome staining. This analysis confirmed a significant increased fibrosis in the hearts derived from the TAC-operated mice, with JDP2-KO mice exhibiting the highest fibrosis levels (Fig. 2G and H). We next used in situ cell death staining to examine apoptosis in TAC operated heart sections. This analysis revealed a significant increase in the number of apoptosis positive cells in heart sections derived from JDP2-KO mice compared with wild type and ATF3-KO counterparts (Fig. 2I). The increase in apoptosis is partially explained by the reduced Bcl2/Bax ratio in JDP2-KO mice (supplemental Fig. 1).

3.5. JDP2-KO mice display decreased cardiac function following TAC

We next used cardiac MRI, the gold standard for LV function and LV mass assessment. LV mass was significantly higher in TAC-operated mice in all three genotypes as compared with their control counterparts. Wild type and JDP2-KO mice showed similar ventricular mass following TAC, while ATF3-KO mass was only modestly increased (Fig. 3A). In addition, end-diastolic and end-systolic volumes were significantly larger in JDP2-KO mice as compared to both wild type and ATF3-KO mice. ATF3-KO mice displayed the smallest chamber volumes in both end-diastole and end-systole (Fig. 3 A–B). JDP2-KO mice consistently displayed a significantly lower ejection fraction (EF) (EF, Fig. 3 B—C) the highest percentage of deteriorated cardiac dysfunction (47%) compared to wild type and ATF3-KO (30% and 27% respectively). These results are consistent with the reduced cardiac function in JDP2-KO mice found in echocardiographic analysis at four weeks following TAC operation (Supplementary Fig. 2). In contrast, ATF3-KO mice following TAC displayed a similar performance as compared to wild type mice (Fig. 3 and Supplementary Fig. 2). Based on these results and previous findings regarding ATF3 deficiency promoting cardiac dysfunction following TAC [20,21], we sought to determine whether cardiomyocyte specific ATF3 deficiency differs from whole body ATF3-KO following TAC. We used $ATF3^{f/f}$ mice crossed with αMHC-CRE to delete ATF3 in cardiomyocytes. These mice displayed similar EF as compared to control mice ($ATF3^{f/f}$) but an attenuated increase in diastolic and systolic volumes and ventricular mass (Supplementary Fig. 3 A–B).

3.6. bZIP repressor compensation paradigm

We next examined the expression of JDP2 and ATF3 in control and TAC operated mice using qRT-PCR. Both JDP2 and ATF3 expression is elevated by 2–3 fold at 8 weeks following TAC procedure (Fig. 4 A-B). Consistently, RNAseq of TAC-operated wild type mice showed that JDP2 and ATF3 transcription is induced to maximal levels (2–3 fold) already at first week and remains constantly elevated until eighth week [30]. Interestingly, the levels of either JDP2 or ATF3 were significantly increased following the absence of its counterpart gene in the hearts derived from control mice (Fig. 4 A–B). Previous studies suggested a role of p38 signaling pathway in the adaptive response in TAC-induced cardiac hypertrophy [31]. Therefore, we studied the TAC induced changes in the MAPK tier and found that all three MAPKs signaling pathway are being significantly activated following TAC operation (Fig. 4 C—F). This is indicated by the increased ratio of the corresponding phospho-MAPK/

A

	Control			TAC		
	Wt	ATF3-KO	JDP2-KO	Wt	ATF3-KO	JDP2-KO
LVEDV, μl	55.3 ± 3.9	58.0 ± 4.2	65.7 ± 3.3	67.9 ± 2.2	59.5 ± 3.4	72.0 ± 3.7†
LVESV, μl	25.8 ± 0.11	24.7 ± 1.7	26.7 ± 1.5	42.0 ± 3.4*	35.2 ± 2.5*	49.4 ± 3.7*†
LV mass, mg	76.3 ± 5.3	73.9 ± 5.0	71.14 ± 2.7	120.7 ± 5.2*†	97.2 ± 5.5*	118.6 ± 6.0*†

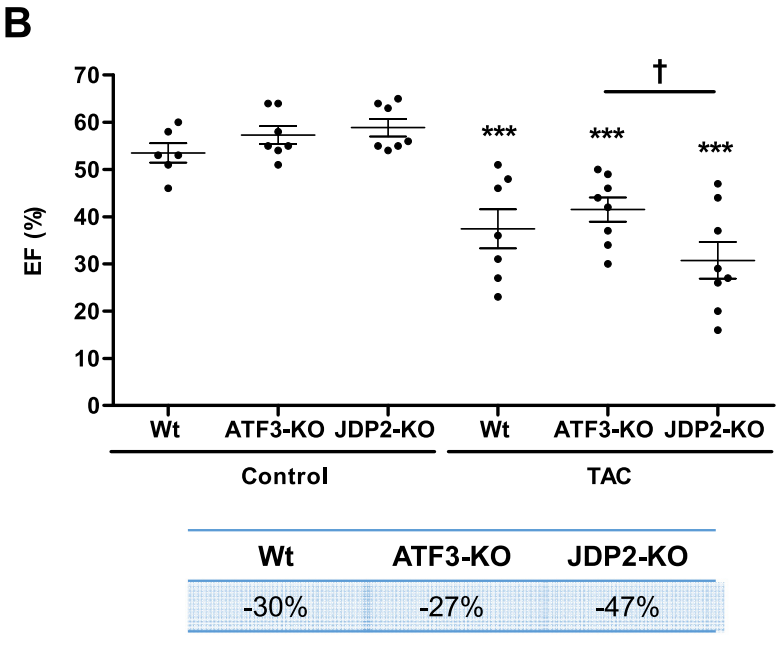

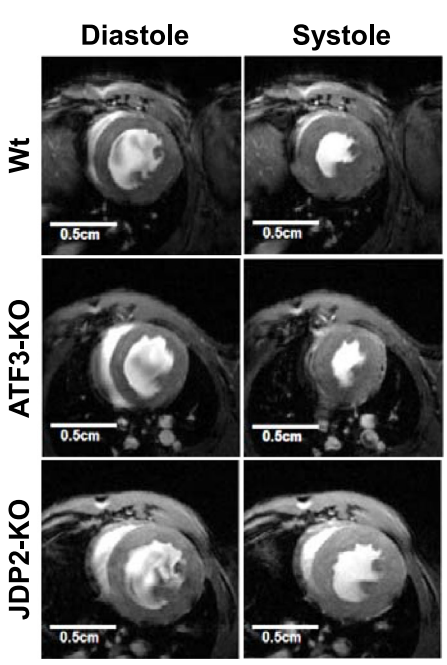

Fig. 3. JDP2-KO mice present deteriorated heart function following TAC. Cardiac hypertrophy was induced by pressure overload (TAC). Following 8 weeks of TAC, left ventricular cardiac volumes, mass and function were examined by a cardiac MRI. (A) The following parameters were measured: left ventricular (LV) mass and left ventricular end-diastolic (LVEDV) and left ventricular end-systolic volume (LVESV). (B) Heart function was assessed by calculating percentage of ejection fraction (EF) according to: EF (%) = [(LVEDV − LVESV) / LVEDV] * 100. The percentage change following TAC for each genotype is shown at the bottom. (C) Representative images of mid-ventricular short-axis slice at peak diastole and systole. The results represent the means ± SE (n = 6–8/group). ***$P \le 0.05$; control vs. TAC, †$P \le 0.05$, difference between genotypes.

Please cite this article as: R. Kalfon, et al., c-Jun dimerization protein 2 (JDP2) deficiency promotes cardiac hypertrophy and dysfunction in response to pressure overload, Int J Cardiol (2017), http://dx.doi.org/10.1016/j.ijcard.2017.08.074

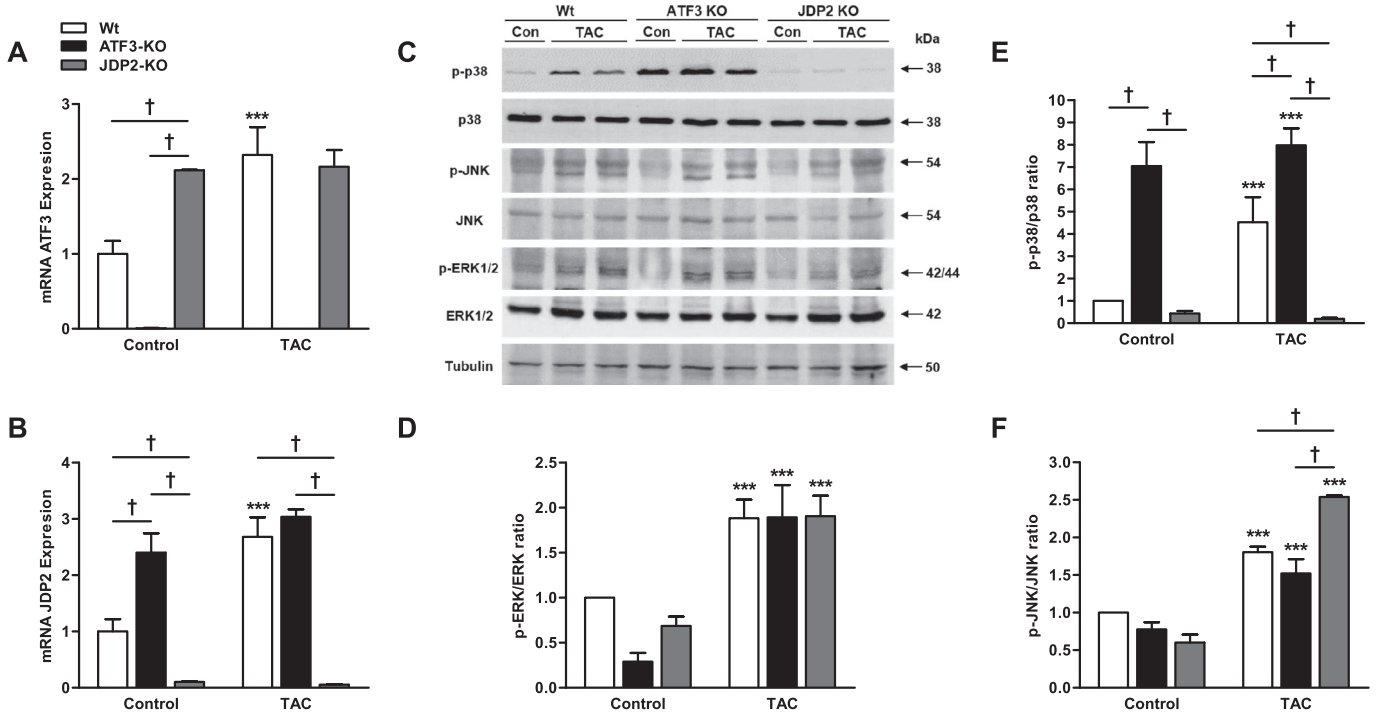

Fig. 4. The bZIP repressor compensation paradigm. mRNA was extracted from ventricles of control and TAC-operated mice and the expression levels of the (A) ATF3 and (B) JDP2 were measured by qRT-PCR. Expression levels are presented as relative values (compared to wild type control mice, determined as 1). The results represent the means ± SE (n = 6–8/group). (C) Western blot analysis of heart lysate derived from the indicated genotypes with the indicated antibodies. (D–F) Densitometric analysis of Western blot shown in C is presented as means ratio of the corresponding phospho-protein to total protein ± SE (compared to wild type control, determined as 1, $n = 4$/group). (D) pERK/ERK (E) pp38/p38 (F) pJNK/JNK. $^{***}P \le 0.05$, control vs. TAC; $^{\dagger}P \le 0.05$ difference between genotypes. The results represent the mean ± SE (n = 6–8/group).

MAPK following TAC. While phospho-ERK ratio is elevated following TAC in all genotypes to similar extent (Fig. 4D), phospho-JNK ratio is significantly elevated in lysate derived from JDP2-KO mice as compared to wild type and ATF3-KO mice (Fig. 4F). Interestingly, lysate derived from JDP2-KO mice showed no phospho-p38 activity in both control and TAC-derived lysates (Fig. 4 C–D). The lack of phospho-p38 activity could be partially explained by the significant loss of MEK6, the p38 upstream regulator, in JDP2-KO mice following TAC (Supplementary Fig. 4 A–B). Collectively, the increase in ATF3 expression level in JDP2-KO mice is consistent with suppression of MEK6 transcription and reduction of the p38 kinase activity following TAC. This suggests the possible role of ATF3 in the maladaptive cardiac remodeling processes following the TAC pressure overload model.

4. Discussion

The role of the bZIP protein superfamily in cardiac remodeling and hypertrophy is well documented. However, since the bZIP family is composed of numerous proteins, the precise role of each member of the family is difficult to interpret. In the heart, the role of the bZIP transcription factors is studied mainly using whole body KO and cardiac specific transgenic mice. In this manuscript, we used whole body KO of both JDP2 and ATF3 as well as cardiac specific ATF3-KO. We analyzed the consequence in control healthy mice as well as mice following stress, using a pressure overload model TAC.

In the absence of stress, the hearts derived from JDP2-KO and ATF3-KO mice display a distinct gene expression pattern that partially resembled a remodeled heart. This includes hypertrophic, fibrosis and inflammatory markers. Yet, only JDP2-KO mice display statistically significant higher Vw/Bw weight ratio. Collectively, we conclude that JDP2 expression is important to maintain homeostasis in the heart and preserve cardiac size and function during normal growth. The lack of ATF3, on the other hand, demonstrates a much milder outcome on cardiac remodeling in non-stressed mice. The latter is consistent with the notion that ATF3 is an immediate early gene and its expression is induced only following stress. Yet, chronic loss of ATF3 even in un-stressed mice display gene expression alterations, suggesting that even low levels of ATF3 expression play a role in promoting long term cardiac remodeling processes.

The significance of JDP2 and ATF3 expression for heart function is highlighted following stress, as simulated by TAC, a pressure overload model. Whereas following TAC the loss of JDP2 results in worsening of cardiac function, the loss of ATF3 is consistent with amelioration of cardiac function and reduced cardiac remodeling processes. Our studies show that TAC-operated ATF3-KO mice display reduced Vw/Bw ratio, lower level of expression of hypertrophic markers, reduced fibrosis and most importantly, attenuated cardiac dysfunction compared to TAC-operated JDP2-KO mice. Following a phenylephrine infusion pressure overload model, we observed a similar protective phenotype i.e., loss of ATF3 expression resulted in reduced cardiac remodeling processes [18,19]. In addition, we have shown that chronic ATF3 expression in the adult heart results in a hypertrophic phenotype leading to cardiac dysfunction [16]. Interestingly, here we showed that elevated ATF3 expression found in JDP2-KO mice is correlated with deterioration in cardiac outcome. Collectively, we conclude that chronic ATF3 expression in the heart is maladaptive and results in cardiac dysfunction. Importantly, heart failure patients display high cardiac levels of ATF3 expression as compared to healthy individuals. In this regard, we hypothesize that chronic ATF3 expression in heart failure patients is maladaptive and therefore is a bone fide drug target to improve cardiac function in these individuals.

In this manuscript, we described a unique bZIP repressor compensation mechanism by which JDP2 and ATF3 regulate the expression level of the other gene. ATF3 is elevated upon loss of JDP2 expression- a potential explanation for the observed cardiac hypertrophy. On the other hand, loss of ATF3 expression resulted in elevated levels of JDP2 which did not lead to a significant deterioration of cardiac function as compared with wild type mice. Thus a delicate balance mechanism exists

Please cite this article as: R. Kalfon, et al., c-Jun dimerization protein 2 (JDP2) deficiency promotes cardiac hypertrophy and dysfunction in response to pressure overload, Int J Cardiol (2017), http://dx.doi.org/10.1016/j.ijcard.2017.08.074

between JDP2 and ATF3. However, although JDP2 and ATF3 are highly similar in the bZIP domain and share multiple cellular functions, the compensation mechanism in their expression demonstrate that these genes may be redundant during normal growth but display distinct cellular functions following stress. A case in point is the activation of MAPK signaling pathway. Our analysis clearly demonstrates that the lack of ATF3 promotes activation of the p38 kinase, while in the absence of JDP2, p38 kinase activation is completely abrogated. This result is consistent with the previously reported role of p38 signaling pathway in the adaptive response to TAC [31,32]. In JDP2-KO mice ATF3 transcription is elevated while MEK6 transcription is suppressed leading to dampening of the p38 kinase signaling pathway and a worse heart outcome phenotype. Furthermore, whereas ATF3 is known to promote apoptosis in β cells [23], JDP2 expression attenuates the appearance of apoptotic cardiomyocytes both in vitro [17] and in vivo (Fig. 2I).

Previous studies suggest that ATF3 deficiency promotes cardiac remodeling processes and deterioration of cardiac function [20,21]. Here we provide evidence that is consistent with the conclusion that ATF3 expression promotes, rather than inhibits, cardiac maladaptive remodeling processes. Thus, although we used the same C57Bl/6 ATF3-KO mice [23] and identical pressure overload model, our results are consistent with an opposite conclusion. It should be noted that the cardiac stress induced using the TAC protocol in the different labs results in heart hypertrophic growth in wild type mice to a similar Vw/Bw ratio [20,21]. The only apparent difference is the time of analysis. While we sacrificed the mice eight weeks following TAC, the other studies analyzed the mice four weeks following TAC. It is possible that ATF3 plays an adaptive role during the acute, compensatory period whereas ATF3 expression turns into a maladaptive role when expression becomes chronic. Further analysis is required to fully reveal the dual role of ATF3 in cardiac remodeling. Understanding the seemingly opposite results using the same experimental model is a crucial step to further elucidate the potential use of bZIP repressor inhibitors for the treatment of heart failure patients.

Supplementary data to this article can be found online at http://dx.doi.org/10.1016/j.ijcard.2017.08.074.

Funds

This work was partially supported by: Mars Pittsburgh Fund for Medical Research and Israel Science Foundation grant 731/17 to A.A.

Conflict of interest

The authors report no relationships that could be construed as a conflict of interest.

Acknowledgments

The authors wish to thank Dr. Lilach Koren and Dr. Sharon Aviram, Mr. Elad Prinz and Mr. Tal Kahn for helpful discussion, Maya Holdengreber and Lior Liba from the BCF Bioimaging Center (Faculty of Medicine, Technion) for their assistance with imaging and image analysis and Dr. Liat Linde from the Genomics Unit for assistance in RNAseq data analysis.

References

[1] A. Aronheim, E. Zandi, H. Hennemann, S. Elledge, M. Karin, Isolation of an AP-1 repressor by a novel method for detecting protein-protein interactions, Mol. Cell. Biol. 17 (1997) 3094–3102.
[2] S. Katz, R. Heinrich, A. Aronheim, The AP-1 repressor, JDP2, is a bona fide substrate for the c-Jun N- terminal kinase, FEBS Lett. 506 (2001) 196–200.
[3] I. Darlyuk-Saadon, K. Weidenfeld-Baranboim, K.K. Yokoyama, T. Hai, A. Aronheim, The bZIP repressor proteins, c-Jun dimerization protein 2 and activating transcription factor 3, recruit multiple HDAC members to the ATF3 promoter, Biochim. Biophys. Acta 1819 (2012) 1142–1153.
[4] K. Weidenfeld-Baranboim, K. Bitton-Worms, A. Aronheim, TRE-dependent transcription activation by JDP2-CHOP10 association, Nucleic Acids Res. 36 (2008) 3608–3619.
[5] S.E. Wardell, V. Boonyaratanakornkit, J.S. Adelman, A. Aronheim, D.P. Edwards, Jun dimerization protein 2 functions as a progesterone receptor N-terminal domain coactivator, Mol. Cell. Biol. 22 (2002) 5451–5566.
[6] M.H. Tsai, K. Wuputra, Y.C. Lin, C.S. Lin, K.K. Yokoyama, Multiple functions of the histone chaperone Jun dimerization protein 2, Gene 590 (2016) 193–200.
[7] K. Weidenfeld-Baranboim, T. Hasin, I. Darlyuk, R. Heinrich, O. Elhanani, J. Pan, et al., The ubiquitously expressed bZIP inhibitor, JDP2, suppresses the transcription of its homologue immediate early gene counterpart, ATF3, Nucleic Acids Res. 37 (2009) 2194–2203.
[8] T. Hasin, O. Elhanani, Z. Abassi, T. Hai, A. Aronheim, Angiotensin II signaling upregulates the immediate early transcription factor ATF3 in the left but not the right atrium, Basic Res. Cardiol. 106 (2011) 175–187.
[9] Z.G. Ma, W.Y. Wei, S.C. Xu, W.B. Zhang, J. Dai, Q.Z. Tang, ATF3: A potential target for cardiac maladaptive remodeling, Int. J. Cardiol. 202 (2016) 50–51.
[10] J. Yang, C.J. Yang, J. Yang, Z.X. Fan, ATF3: A promotion effect or a inhibition effect in cardiac maladaptive remodeling, Int. J. Cardiol. 201 (2015) 245–246.
[11] H. Zhou, Y. Yuan, J. Ni, H. Guo, W. Deng, Z.Y. Bian, et al., Pleiotropic and puzzling effects of ATF3 in maladaptive cardiac remodeling, Int. J. Cardiol. 206 (2016) 87–88.
[12] R. Kalfon, L. Koren, A. Aronheim, ATF3, a novel cardiac therapeutic target: beneficial or harmful? Int. J. Cardiol. 234 (2017) 124.
[13] L. Koren, Y. Shaked, A. Aronheim, Response letter: "ATF3: a promoter or inhibitor of cardiac maladaptive remodeling", Int. J. Cardiol. 201 (2015) 692.
[14] Y. Okamoto, A. Chaves, J. Chen, R. Kelley, K. Jones, H.G. Weed, et al., Transgenic mice with cardiac-specific expression of activating transcription factor 3, a stress-inducible gene, have conduction abnormalities and contractile dysfunction, Am. J. Pathol. 159 (2001) 639–650.
[15] I. Kehat, R. Heinrich, O. Ben-Izhak, H. Miyazaki, J.S. Gutkind, A. Aronheim, Inhibition of basic leucine zipper transcription is a major mediator of atrial dilatation, Cardiovasc. Res. 70 (2006) 543–554.
[16] L. Koren, O. Elhanani, I. Kehat, T. Hai, A. Aronheim, Adult cardiac expression of the activating transcription factor 3, ATF3, Promotes Ventricular Hypertrophy. PloS ONE. 8 (2013), e68396.
[17] C. Hill, A. Wurfel, J. Heger, B. Meyering, K.D. Schluter, M. Weber, et al., Inhibition of AP-1 signaling by JDP2 overexpression protects cardiomyocytes against hypertrophy and apoptosis induction, Cardiovasc. Res. 99 (2013) 121–128.
[18] L. Koren, D. Alishekevitz, O. Elhanani, A. Nevelsky, T. Hai, I. Kehat, et al., ATF3-dependent cross-talk between cardiomyocytes and macrophages promotes cardiac maladaptive remodeling, Int. J. Cardiol. 198 (2015) 232–240.
[19] L. Koren, U. Barash, Y. Zohar, N. Karin, A. Aronheim, The cardiac maladaptive ATF3-dependent cross-talk between cardiomyocytes and macrophages is mediated by the IFNgamma-CXCL10-CXCR3 axis, Int. J. Cardiol. 228 (2016) 394–400.
[20] H. Zhou, D.F. Shen, Z.Y. Bian, J. Zong, W. Deng, Y. Zhang, et al., Activating transcription factor 3 deficiency promotes cardiac hypertrophy, dysfunction, and fibrosis induced by pressure overload, PLoS One 6 (2011), e26744.
[21] Y. Li, Z. Li, C. Zhang, P. Li, Y. Wu, C. Wang, et al., Cardiac fibroblast-specific activating transcription factor 3 protects against heart failure by suppressing MAP2K3-p38 signaling, Circulation 135 (2017) 2041–2057.
[22] R. Kalfon, L. Koren, S. Aviram, O. Schwartz, A. Aronheim, ATF3 expression in cardiomyocytes preserves homeostasis in the heart and controls peripheral glucose tolerances, Cardiovasc. Res. 113 (2017) 134–146.
[23] M.G. Hartman, D. Lu, M.L. Kim, G.J. Kociba, T. Shukri, J. Buteau, et al., Role for activating transcription factor 3 in stress-induced beta-cell apoptosis, Mol. Cell. Biol. 24 (2004) 5721–5732.
[24] C. Jin, K. Kato, T. Chimura, T. Yamasaki, K. Nakade, T. Murata, et al., Regulation of histone acetylation and nucleosome assembly by transcription factor JDP2, Nat. Struct. Mol. Biol. 13 (2006) 331–338.
[25] C.C. Wolford, S.J. McConoughey, S.P. Jalgaonkar, M. Leon, A.S. Merchant, J.L. Dominick, et al., Transcription factor ATF3 links host adaptive response to breast cancer metastasis, J. Clin. Invest. 123 (2013) 2893–2906.
[26] R. Agah, P.A. Frenkel, B.A. French, L.H. Michael, P.A. Overbeek, M.D. Schneider, Gene recombination in postmitotic cells. Targeted expression of Cre recombinase provokes cardiac-restricted, site-specific rearrangement in adult ventricular muscle in vivo, J. Clin Invest 100 (1997) 169–179.
[27] H.A. Rockman, R.S. Ross, A.N. Harris, K.U. Knowlton, M.E. Steinhelper, L.J. Field, et al., Segregation of atrial-specific and inducible expression of an atrial natriuretic factor transgene in an in vivo murine model of cardiac hypertrophy, Proc. Nat. Acad Sci USA 88 (1991) 8277–8281.
[28] A.C. de Almeida, R.J. van Oort, X.H. Wehrens, Transverse aortic constriction in mice, J Vis Exp. 38 (2010) http://dx.doi.org/10.3791/1729.
[29] E. Heiberg, J. Sjogren, M. Ugander, M. Carlsson, H. Engblom, H. Arheden, Design and validation of segment-freely available software for cardiovascular image analysis, BMC Med. Imaging 10 (2010) 1.
[30] X. Ma, L. Gao, G. Karamanlidis, P. Gao, C.F. Lee, L. Garcia-Menendez, et al., Revealing pathway dynamics in heart diseases by analyzing multiple differential networks, PLoS Comp. Biol. 11 (2015), e1004332.
[31] J.C. Braz, Bueno OF, Q. Liang, B.J. Wilkins, Y.S. Dai, S. Parsons, et al., Targeted inhibition of p38 MAPK promotes hypertrophic cardiomyopathy through upregulation of calcineurin-NFAT signaling, J. Clin. Invest. 111 (2003) 1475–1486.
[32] K. Nishida, O. Yamaguchi, S. Hirotani, S. Hikoso, Y. Higuchi, T. Watanabe, et al., p38alpha mitogen-activated protein kinase plays a critical role in cardiomyocyte survival but not in cardiac hypertrophic growth in response to pressure overload, Mol. Cell. Biol. 24 (2004) 10611–10620.

Please cite this article as: R. Kalfon, et al., c-Jun dimerization protein 2 (JDP2) deficiency promotes cardiac hypertrophy and dysfunction in response to pressure overload, Int J Cardiol (2017), http://dx.doi.org/10.1016/j.ijcard.2017.08.074